



저작자표시-비영리-변경금지 2.0 대한민국

이용자는 아래의 조건을 따르는 경우에 한하여 자유롭게

- 이 저작물을 복제, 배포, 전송, 전시, 공연 및 방송할 수 있습니다.

다음과 같은 조건을 따라야 합니다:



저작자표시. 귀하는 원저작자를 표시하여야 합니다.



비영리. 귀하는 이 저작물을 영리 목적으로 이용할 수 없습니다.



변경금지. 귀하는 이 저작물을 개작, 변형 또는 가공할 수 없습니다.

- 귀하는, 이 저작물의 재이용이나 배포의 경우, 이 저작물에 적용된 이용허락조건을 명확하게 나타내어야 합니다.
- 저작권자로부터 별도의 허가를 받으면 이러한 조건들은 적용되지 않습니다.

저작권법에 따른 이용자의 권리는 위의 내용에 의하여 영향을 받지 않습니다.

이것은 [이용허락규약\(Legal Code\)](#)을 이해하기 쉽게 요약한 것입니다.

[Disclaimer](#)

공학석사학위논문

**Parameter Identification of Structures
under Earthquake Excitations
Using Adaptive Particle Filter and Ensemble
Learning Method**

적응형 파티클 필터와 앙상블 학습 기법을 이용한
지진동 응답 기반 구조 시스템 파라미터 추정

2019 년 2 월

서울대학교 대학원

건설환경공학부

김 민 규

**Parameter Identification of Structures under
Earthquake Excitations Using Adaptive Particle
Filter and Ensemble Learning Method**




적응형 파티클 필터와 앙상블 학습 기법을 이용한
지진동 응답 기반 구조 시스템 파라미터 추정

지도 교수 송 준 호

이 논문을 공학석사 학위논문으로 제출함
2019 년 2 월

서울대학교 대학원
건설환경공학부
김 민 규

김민규의 공학석사 학위논문을 인준함
2019 년 1 월

위 원 장	<u>김 호 경</u>	
부위원장	<u>송 준 호</u>	
위 원	<u>문 국 호</u>	

Abstract

Parameter Identification of Structures under Earthquake Excitations Using Adaptive Particle Filter and Ensemble Learning Method

Kim, Minkyu

Department of Civil & Environmental Engineering

The Graduate School

Seoul National University

Social demand for accurate post-evaluation and monitoring of infrastructure has been increasing since the earthquake in Gyeongju in 2016 and Pohang in 2017. To increase the accuracy of post-evaluation and monitoring, an accurate estimation of system equation, (i.e. system parameters) is required.

Among other machine learning methods based on the data assimilation, a sampling-based particle filter was used to estimate systems with strong nonlinearity, which achieved high accuracy in estimation of system parameters. However, damage, such as stiffness degradation, that occurs during extreme events can cause sudden changes in the system parameters. The existing methods have shown poor performance in this case because they assume that the system parameters are

constant over the time.

In this study, an adaptive particle filter is introduced to accurately estimate system parameters that suddenly change in extreme events. The adaptive particle filter is intended to artificially increase the parameter estimation noise of the particle filter according to the situation in order to estimate the system parameters that change over time as damage occurs. Furthermore, we propose modified adaptive particle filter that allocates different parameter estimation noises to each degree of freedom based on measurements.

However, the adaptive particle filter has the problem of increasing the variance of estimation. Therefore, this study introduces an ensemble learning method that obtains the final estimate by aggregating estimates from usable parallel algorithms. In this study, Bootstrap Aggregating or Bagging is used, which aggregates estimates with the same weight from parallel algorithms to obtain the final estimate.

We expect that a more accurate and effective post-evaluation and monitoring of infrastructures can be carried out, and effective maintenance can be possible through accurate information about the damaged element obtained from the proposed method.

Keywords: earthquake disaster, structural response, system identification, data assimilation, adaptive particle filter, ensemble learning method

Student Number: 2017-20456

TABLE OF CONTENTS

LIST OF FIGURE	v
1. Introduction	1
1.1. Research Background	1
1.2. Research Objectives and Scope	6
1.3. Outline	8
2. Theoretical Background	9
2.1. Estimation in the State Space.....	9
2.2 Particle Filter.....	13
2.3 Adaptive Particle Filter	21
3. Proposed Modified Adaptive Particle Filter with Ensemble Learning Method	26
3.1. Modified Adaptive Particle Filter	26
3.2 Ensemble Learning Method.....	31

4. Verification of Proposed Method	36
4.1.Numerical Example	36
4.1.1 Target Structural System	36
4.1.2 Ground Acceleration.....	38
4.1.3 Stiffness Degradation	39
4.2. Verification Results and Discussion.....	42
4.2.1 Original Particle Filter.....	42
4.2.2 Modified Adaptive Particle Filter.....	44
4.2.3 Modified Adaptive Particle Filter with Bagging	45
5. Conclusion.....	53
REFERENCE	55
국문 초록	58

TABLE OF CONTENTS

Figure 1.1 Severe damage caused by the Pohang earthquake	5
Figure 1.2 Local failure of bridge caused by the Sichuan earthquake	5
Figure 2.1 Flow chart of particle filter algorithm.....	19
Figure 2.2 Systematic resampling based on uniform resampler.....	19
Figure 2.3 Schematized algorithm of particle filter.....	20
Figure 2.4 Flow chart of adaptive particle filter.....	25
Figure 3.1 Simple example showing how to calculate adaptive coefficient in modified adaptive particle filter.....	30
Figure 3.2 Simple concept of ensemble learning method	35
Figure 3.3 Estimation process of modified adaptive particle filter with Bagging method.....	35
Figure 4.1 Target Structure (10 story shear building).....	40
Figure 4.2 Ground acceleration record of El Centro earthquake.....	40
Figure 4.3 Stiffness degradation in k_1 , k_2 and k_3	41
Figure 4.4 Displacement, velocity and acceleration estimation of degree of freedom 1 (upper) and 10 (lower) from particle filter	47

Figure 4.5 Parameter estimation of (upper) $k_1 \sim k_5$ and $k_6 \sim k_{10}$ (lower)	
from particle filter	48
Figure 4.6 Displacement, velocity and acceleration estimation of degree of	
freedom 1 (upper) and 10 (lower) from modified adaptive particle	
filter.....	49
Figure 4.7 Parameter estimation of (upper) $k_1 \sim k_5$ and $k_6 \sim k_{10}$ (lower)	
from modified adaptive particle filter	50
Figure 4.8 Change in values of $\lambda_{i,k}$ over time	51
Figure 4.9 Parameter estimation of (upper) $k_1 \sim k_5$ and $k_6 \sim k_{10}$ (lower)	
from modified adaptive particle filter with Bagging method	52

1. Introduction

1.1. Research Background

In 2016 and 2017, major earthquakes with 5.8 and 5.4 magnitude have occurred in Gyeongju and Pohang, respectively. As a result, many damages occurred as shown in Figure 1.1. South Korea had little experience in such a large-scale earthquake, and there was the lack of countermeasure to deal with the earthquake disaster. Accordingly, social interest and concerns about seismic disasters greatly increased, and the need for the post-evaluation of infrastructure after the earthquake and a study of Structural Health Monitoring (SHM) increased significantly.

System identification is essential for post-evaluation of a structure. However, accurate system identification requires a method that requires a lot of money and time, such as field investigation. In this way, it is impossible to respond quickly in the event of an earthquake. Therefore, it is essential with the limited information to forecast an indirect estimation of the condition of an infrastructure, such as the response of a structure at the time of the earthquake (Bisht & Singh, 2014).

In the event of an earthquake, the structure suffers from a high degree of displacement in a very short period. Therefore, system parameters can change rapidly in a short period such as stiffness degradation due to local damage. Figure 1.2 shows the local failure of the bridge in the Xingyiu area of China. The bridge was damaged by the Sichuan earthquake in 2008. Change in the system parameters

has a serious effect on the bridge structure, such as the degradation of the structural performance and loss of life. If damage to the structure is not identified in time and the damaged structure is used continuously without any maintenance, the structure may collapse leading to serious secondary damage after the earthquake. However, change in these system parameters is difficult to identify without going through field investigations, such as destructive or non-destructive testing.

As signal processing techniques develop, frequency domain methods such as Fast Fourier Transform (FFT) have been widely used in SHM as the indirect estimation. However, the frequency domain method has a disadvantage. The measurement noise causes an ill-conditioned problem in the estimated solution has non-stability and non-uniqueness (Alvin *et. al.*, 2003). These issues encourage researchers to consider time domain methods such as the Kalman Filter (KF) (Yang *et. al.*, 2006). KF is a recursive filter that estimates the state of linear dynamics, which has the advantage of enabling real-time online estimation based on the measurements.

Especially, the indirect estimation of system parameters through machine learning methods is receiving attention. The aforementioned KF is known to be the most accurate estimator in linear and Gaussian system. However, most of the structural systems are non-linear and non-Gaussian. Many versions of the KF have been developed, such as the Extended Kalman Filter (EKF) and Unscented Kalman Filter (UKF). These are designed and modified to estimate nonlinear system estimation (Simon, 2006). Modified versions of KF are widely used in a various engineering fields in these days.

However, the KF-based methods are ineffective in non-Gaussian systems

because they assume a Gaussian system. Hence, studies on the Particle Filter (PF), developed for estimating nonlinear Gaussian systems, were conducted, which showed high accuracy in estimating system parameters. Because PF is based on a sampling method, it also has the advantage of being able to estimate complicated probability distributions.

However, existing methods assume that system parameters do not change over time. Thus, it is difficult to estimate parameters correctly when system parameters change, such as stiffness degradation. Accordingly, Liu *et. al.* (2005) proposed the Adaptive Particle Filter (APF) to estimate parameters that change over time. The APF detects when a system change occurs and artificially increases the parameter estimation noise at that moment. The increase of noise enables the PF to estimate system parameters that change over time. In this study, we propose that the modified APF can improve the method for the increase of noise.

The APF has the advantage of increasing noise, which helps the PF to adapt quickly to the situation. However, at the same time, the variance of estimation is significantly increased due to the noise increased by adaptive coefficient. To reduce the variance of estimation, an ensemble learning method is often introduced to the machine learning problems. The ensemble learning method combines each estimate from the executable algorithms to obtain the final estimate. It is known that the variance of estimation obtained from the ensemble learning method is always smaller than the one obtained from a single algorithm (Nasrabadi, 2007).

In this study, we use bootstrap aggregation (bagging) to give equal weights to the estimates from each algorithm to obtain the final estimate. Therefore, this study improves an accuracy of estimation by reducing the variance while estimating

parameters that change over time.



**Figure 1.1 Severe damage caused by the Pohang earthquake
(Staff and agencies, 2017)**



**Figure 1.2 Local failure of bridge caused by the Sichuan earthquake
("Images from the Sichuan," 2009)**

1.2. Research Objectives and Scope

This study has two main objectives. First, for the accurate estimation of the process of the stiffness degradation, which occurred during an earthquake disaster in real time, this study suggests the ways of improving the existing adaptive particle filter. The adaptive particle filter uses the method to increase the parameter estimation noise through a single adaptive coefficient. However, this method has a problem in that the variance of estimation greatly increases due to the increase in all components of the noise vector. Therefore, this study proposes the modified adaptive particle filter. In the modified adaptive particle filter, the noise vector is multiplied by a vector consisting of several different adaptive coefficients. That is, each component of the noise is increased by different adaptive coefficients. This method helps the adaptive particle filter to estimate time-varying parameters with small variance.

Second, this study proposes a method that combine estimates from parallel algorithms by using bagging, which is one of the ensemble learning method, to reduce the variance of estimation and to increase the accuracy of the estimation in the modified adaptive particle filter. Although the modified adaptive particle filter decreases the variance in comparison to the existing methods, it still has a large variance of estimation because the method is based on the increase of noise. Therefore, bagging combines the estimates from several modified adaptive particle filters to obtain the final estimate.

This study is divided into two parts. The first part provides a theoretical explanation about state estimation, particle filter and adaptive particle filter, which

are the basis of the proposed methodology. This study also provide a theoretical explanation about the proposed modified adaptive particle filter with the ensemble learning method.

The second part validates the method proposed in the first part with a numerical example using actual seismic data. In the numerical example, we assume that the earthquake caused the stiffness degradation in the structure. This proves that the proposed method has better estimation performance than the existing methods.

1.3. Outline

Chapter 1 is the Introductions, which present the research background, objects and scopes and outline. Chapter 2 provides the theoretical background about the state estimation, particle filter, and adaptive particle filter, which are the basis for the method proposed in this study. Chapter 3 presents the modified adaptive particle filter proposed in this study based on the methods presented in Chapter 2. This study also presents theoretical explanations about the introduced ensemble learning method introduced for enhancing the performance of the proposed method and application of the modified adaptive particle filter. Chapter 4 presents a numerical example to validate the proposed method in Chapter 3. In this study, simulations are performed using the linear shear building structures with actual seismic data. This study presents the results of the particle filter, the modified adaptive particle filter and the modified adaptive particle filter using the ensemble learning method for the given numerical example and validates the performance of the proposed methodology. Chapter 5 summarizes the study and provides academic and practical implications, study limitation, and suggestions for future research.

2. Theoretical Background

2.1. Estimation in the State Space

As mentioned in Chapter 1, the time domain method based on machine learning is widely used in the real-time estimation. Among them, the Kalman filter has been widely used since the 1950s in the engineering fields because it is easy to implement.

To estimate the system using the time domain estimator based on the Kalman filter method, the given system needs to be expressed in the state-space representation. The state-space representation is a mathematical model for expressing the physical system in the first-order differential equation through input, output, and state that needs to be estimated. Here, the state refers to a minimum subset of the system variables that can represent the overall system status at any time.

State-space representations can be expressed in linear and nonlinear equations depending on the characteristics of the system. State-space representation of linear systems over continuous time is expressed as Eq. 2.1 and Eq.2.2, and State-space representation of nonlinear systems is expressed as the following Eq. 2.3 and Eq. 2.4. Generally, it is common to assume that noise vectors $\mathbf{w}(t)$ and $\mathbf{v}(t)$ are random noises that follow the Gaussian distribution. However, if the distribution characteristics of $\mathbf{w}(t)$ and $\mathbf{v}(t)$ are known, the non-Gaussian noise also can be used.

$$\dot{\mathbf{x}}(t) = \mathbf{A}\mathbf{x}(t) + \mathbf{B}\mathbf{u}(t) + \mathbf{w}(t) \quad (2.1)$$

$$\mathbf{y}(t) = \mathbf{C}\mathbf{x}(t) + \mathbf{D}\mathbf{u}(t) + \mathbf{v}(t) \quad (2.2)$$

$$\dot{\mathbf{x}}(t) = f(\mathbf{x}(t), \mathbf{u}(t), \mathbf{w}(t)) \quad (2.3)$$

$$\mathbf{y}(t) = h(\mathbf{x}(t), \mathbf{v}(t)) \quad (2.4)$$

In addition, state-space representation of linear systems at discrete times can be expressed as the following Eq. 2.5, Eq. 2.6, Eq. 2.7 and Eq.2.8 for the nonlinear systems.

$$\mathbf{x}_{k+1} = \mathbf{A}\mathbf{x}_k + \mathbf{B}\mathbf{u}_k + \mathbf{w}_k \quad (2.5)$$

$$\mathbf{y}_k = \mathbf{C}\mathbf{x}_k + \mathbf{D}\mathbf{u}_k + \mathbf{v}_k \quad (2.6)$$

$$\mathbf{x}_{k+1} = f(\mathbf{x}_k, \mathbf{u}_k, \mathbf{w}_k) \quad (2.7)$$

$$\mathbf{y}_k = h(\mathbf{x}_k, \mathbf{u}_k, \mathbf{v}_k) \quad (2.8)$$

For a simple example, the linear structure system's equation of motion is expressed as the following Eq. 2.9. The state vector $\mathbf{z}(t)$ can be set with the displacement \mathbf{u} and the speed vector $\dot{\mathbf{u}}$ as shown in Eq. 2.10. Then, the state-space representation of the equation of motion can be written as the linear equation as shown in Eq. 2.11 when all other system parameters are known.

$$\mathbf{M}\ddot{\mathbf{u}}(t) + \mathbf{C}\dot{\mathbf{u}}(t) + \mathbf{K}\mathbf{u}(t) = \mathbf{F}(t) \quad (2.9)$$

$$\mathbf{z}(t) = [\mathbf{u} \quad \dot{\mathbf{u}}]^T \quad (2.10)$$

$$\dot{\mathbf{z}}(t) = \begin{bmatrix} 0 & I_{DOF} \\ -\mathbf{M}^{-1}\mathbf{K} & -\mathbf{M}^{-1}\mathbf{C} \end{bmatrix} \mathbf{z}(t) + \begin{bmatrix} 0 \\ -\mathbf{M}^{-1}\mathbf{F}(t) \end{bmatrix} + \mathbf{w}(t) \quad (2.11)$$

However, when estimating system parameters such as stiffness and damping coefficients, these system parameters need to be added to the state vector, as shown in Eq. 2.12. For this reason, it is unable to express as the linear equation of Eq. 2.11. Therefore, the equation of motion is represented by the nonlinear equation, as shown in Eq. 2.13.

$$\mathbf{z}(t) = [\mathbf{u}(t) \quad \dot{\mathbf{u}}(t) \quad \boldsymbol{\theta}]^T \quad (2.12)$$

$$\dot{\mathbf{z}}(t) = f(\mathbf{z}(t), \mathbf{F}(t), \mathbf{w}_a(t)) \quad (2.13)$$

$\mathbf{w}_a(t)$ is a noise vector containing the original noise vector $\mathbf{w}(t)$ and an added parameter estimation vector $\mathbf{w}_\theta(t)$, which can be written as the following equation.

$$\mathbf{w}_a(t) = [\mathbf{w}(t) \quad \mathbf{w}_\theta(t)]^T \quad (2.14)$$

Because the system parameters are assumed to be constant over time, $\mathbf{w}_\theta(t)$ is set to be small enough. Here, $\mathbf{w}_\theta(t)$ plays a role similar to the learning step size of the machine learning method. Here, setting $\mathbf{w}_\theta(t)$ too large make the estimate diverge. Conversely, if $\mathbf{w}_\theta(t)$ is set too small, the convergence speed may be too slow to converge within a given time period. Therefore, it is important to set an appropriate size of $\mathbf{w}_\theta(t)$. In many studies, it is common to select the value between 0.01% and 1% of the parameter's initial value as the standard

deviation of the distribution of $\mathbf{w}_\theta(t)$.

As explained in Chapter 1, Kalman filter is known as the best estimator for linear and Gaussian systems such as Eq. 2.11. However, Kalman filter is not effective in estimating the non-linear problems such as Eq. 2.13 as well as non-Gaussian systems (Simon, 2006). Therefore, the particle filter, which is an appropriate estimator for the non-linear and non-Gaussian system, is introduced in this study.

2.2. Particle Filter

Many modified versions of Kalman filter have been developed to solve nonlinear problems with Kalman filter that is optimized only for the linear problems. Among them, extended Kalman filter and unscented Kalman filter mentioned in Chapter 1 are widely used in many problems.

The extended Kalman filter is the method that uses the first-order differentiated nonlinear system equation, such as Eq. 2.3 and Eq. 2.4, at the current state of the estimate (Ljung, 1979). However, because it is low-order approximation method, there is a stability problem in that the estimate can be diverged as the nonlinearity of a given system increases (Simon, 2006).

The unscented Kalman filter uses the statistical characteristics of the current estimated states to obtain the final estimate after obtaining the estimates at various points that is called the sigma points. The unscented Kalman filter combines the estimates from the sigma points, which has same values of ensemble mean and variance with the current estimated state (Wan & Van Der Merwe, 2000). However, if the probability distribution of the system has complicated form, it is difficult to estimate them.

The particle filter is developed to solve this kind of problem. The particle filter is a real-time machine learning-based estimation method for state estimation based on Bayesian statistics and the importance sampling method. Unlike the Kalman filter-based methods, the particle filter generates random samples, or particles, from the initial probability distribution, and then updates the state of the

particles recursively using the given information, system equations and measurements. The state and weight of each particle is combined to estimate the state of each time-step and the probability distribution (Chatzi & Smyth, 2009). This is why the particle filter is also known as Bayesian recursive filter. Unlike aforementioned Kalman filter-based methods, the particle filter is based on the sampling method, which has the advantage of approximation of the complicated probability distribution and application to the nonlinear problems.

The particle filter operates based on the recursive Bayesian state estimator. The recursive Bayesian state estimator is a method to update state recursively by obtaining the prior distribution every time step using Bayes' theorem and the system equation, and then obtaining the posterior distribution based on the measurements at that time.

Let us assume that the nonlinear system such as Eq. 2.7 or Eq. 2.8 is given. Here, it is assumed that the initial probability distribution of states, shown in Eq. 2.15, is known regardless of the measurement.

$$p(\mathbf{x}_0 | \mathbf{Y}_0) = p(\mathbf{x}_0) \quad (2.15)$$

Before obtaining measurements at the time step k , the prior distribution of state obtained by updating the state of each particle with the given system equation is written as Eq. 2.16. Here, $p(\mathbf{x}_k | \mathbf{x}_{k-1})$ is obtained from the system equation, and $p(\mathbf{x}_{k-1} | \mathbf{Y}_{k-1})$ is the posterior distribution of the previous step.

$$p(\mathbf{x}_k | \mathbf{Y}_{k-1}) = \int p(\mathbf{x}_k | \mathbf{x}_{k-1}) p(\mathbf{x}_{k-1} | \mathbf{Y}_{k-1}) d\mathbf{x}_{k-1} \quad (2.16)$$

After obtaining the measurement at the time step k , the posterior distribution

obtained by updating the distribution through the likelihood of measurement is written as Eq. 2.17. Here, $p(\mathbf{x}_k | \mathbf{Y}_{k-1})$ is the prior distribution obtained in the previous step $k-1$, and $p(\mathbf{y}_k | \mathbf{x}_k)$ is the likelihood of the measurement obtained in the time step k (Ang & Tang, 2007).

$$p(\mathbf{x}_k | \mathbf{Y}_k) = \frac{p(\mathbf{y}_k | \mathbf{x}_k) p(\mathbf{x}_k | \mathbf{Y}_{k-1})}{\int p(\mathbf{y}_k | \mathbf{x}_k) p(\mathbf{x}_k | \mathbf{Y}_{k-1}) d\mathbf{x}_k} \quad (2.17)$$

As with the recursive Bayesian state estimator, the particle filter also has two main stages, prediction and measurement update, which are shown in Figure 2.1. Before performing the main part of the algorithm, N_p particles are extracted from the initial distribution of state shown in Eq. 2.15. The performance of the particle filter is greatly affected by N_p , and the more complex problem, the larger N_p is needed. If N_p is too small, the estimate can be trapped in the local minima which leads to divergence of estimation, or if N_p is too large, significant computational effort is needed.

First is Prediction step to propagate the state of the initial or previous stage particles to the next time step based on the system equation and the prior distribution. The state propagation of i^{th} particle from time step $k-1$ to k is performed with the system equation shown in Eq. 2.7 and this equation can be rewritten as Eq. 2.18 for each particle.

$$\mathbf{x}_{k,i}^- = f_{k-1}(\mathbf{x}_{k-1,i}^+, \mathbf{u}_{k-1,i}, \mathbf{w}_{k-1,i}) \quad (i = 1, \dots, N_p) \quad (2.18)$$

Second is the measurement update step to estimate the posterior distribution

of state based on the measurement \mathbf{y}_k obtained at the current time step k . As shown in Eq. 2.17, the posterior distribution is proportional to the likelihood of measurement $p(\mathbf{y}_k | \mathbf{x}_k)$. Based on this, particle filter approximates the posterior distribution using the weight of each particle. In addition, since the area below the probability distribution is always one, the weight obtained from likelihood of measurement needs to be normalized to obtain the final value. This can be written as Eq. 2.19 and Eq. 2.20.

$$q_i = p\left[(y_k = y^*) | (x_k = x_{k,i}^-)\right] \quad (2.19)$$

$$q_i = \frac{q_i}{\sum_{j=1}^{N_p} q_j} \quad (2.20)$$

If measurement y_k follows the Gaussian distribution, the weight q_i is proportional to the equation shown in Eq. 2.21 (Simon, 2006).

$$\begin{aligned} q_i &= p\left[(y_k = y^*) | (x_k = x_{k,i}^-)\right] \\ &\sim \frac{1}{(2\pi)^{m/2} |\mathbf{R}|^{1/2}} \exp\left(\frac{-\left[y^* - h(x_{k,i}^-)\right]^T \mathbf{R}^{-1} \left[y^* - h(x_{k,i}^-)\right]}{2}\right) \end{aligned} \quad (2.21)$$

The particle filter repeats these two steps to obtain an optimal estimate at each time step. However, if this process is repeated many times, a few particles take most of the weights in some case. This phenomenon is called the sample deletion. As a result, the estimate is caught on the local minimum and the numerical issues that increase computational cost and make estimation inaccurate are caused in the sampling process.

To solve this problem, a new step called the resampling is introduced. Here,

unweighted particles are resampled proportionately to the size of the previous weights as the number of particles is maintained. That is, particles with large weight are preserved, but particles with large weight are discarded. The resampling is performed when the effective number of N_{eff} is smaller than the threshold N_{thresh} as presented in Eq. 2.22 and Eq. 2.23.

$$N_{eff} = \frac{1}{\sum_{i=1}^{N_p} q_i^2} \quad (2.22)$$

$$N_{eff} = \begin{cases} \leq N_{thresh} & \text{Resample} \\ > N_{thresh} & \text{Accept} \end{cases} \quad (2.23)$$

If N_{eff} is satisfied with the criteria for resampling, the resampling is performed based on a uniform sampling procedure to remove particles with small weight. The resampling extracts new particles with uniform weight from an approximated discrete posterior distribution.

$$p(\mathbf{x}_k | \mathbf{Y}_k) \approx \sum_{i=1}^{N_p} q_i \delta(\mathbf{x}_k - \mathbf{x}_{k,i}^+) \quad (2.24)$$

There are many types of resampling. Among them, multinomial, systematic, and residual method resampling are most often used. In this study, the systematic resampling is used. The systematic resampling is performed in the following order (Candy, 2016). This is illustrated in Figure 2.2.

1. N_p -ordered variates \hat{u}_j are generated as the following equation, by

inverse transforming a uniform sampler:

$$\hat{u}_j = u_j + \frac{i-1}{N_p} \text{ for } i, j = 1, \dots, N_p \text{ and } u_k \sim U\left(0, \frac{1}{N_p}\right) \quad (2.25)$$

2. For $j = 1, \dots, N_p$, the existing particle $\mathbf{x}_{k,i}$ is replaced by $\mathbf{x}_{k,i}$ when \hat{u}_j is larger than the sequential sum of q_i . Here, new weights are uniform,

$$q_j = 1 / N_p.$$

The entire particle filter algorithm as explained so far is schematized in Figure 2.3. This figure illustrates that how weights of particles change repeating main steps and resampling, and approximate prior and posterior distribution.

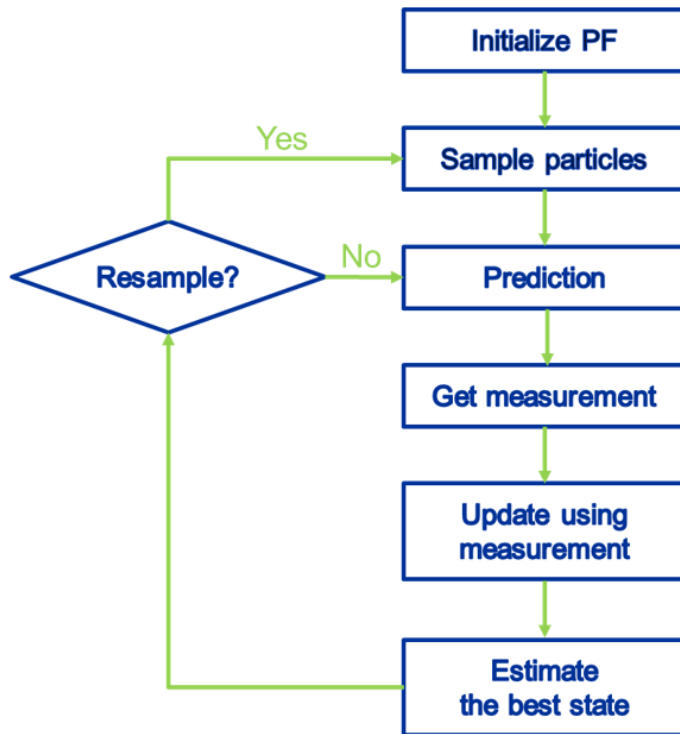


Figure 2.1 Flow chart of particle filter algorithm

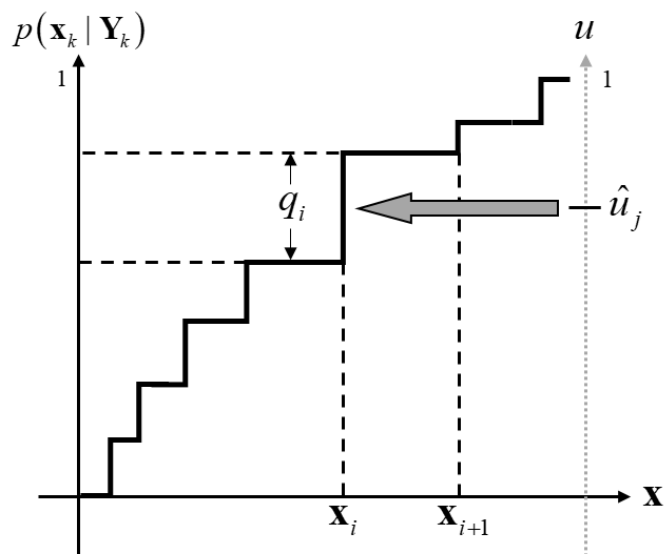


Figure 2.2 Systematic resampling based on uniform resampler

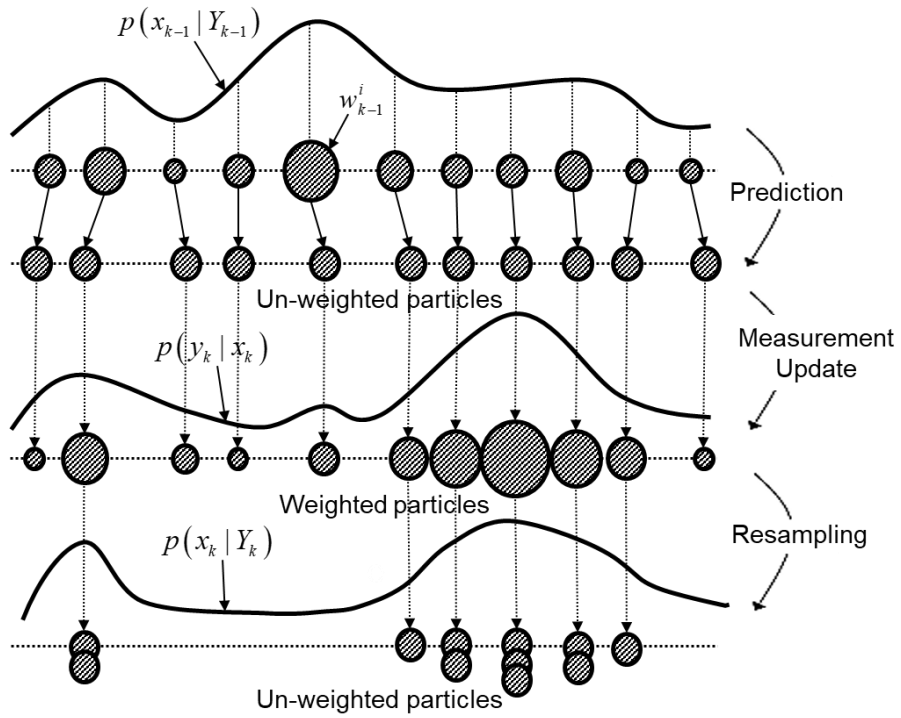


Figure 2.3 Schematized algorithm of particle filter

2.3. Adaptive Particle Filter

The particle filter explained in the previous section shows better performance in nonlinear and non-Gaussian problems than the Kalman filter-based methods. Especially, the particle filter is effective in estimating time-invariant system parameters, shown in Eq. 2.13. This helps the particle filter to enable effective system identification through indirect estimation for complex systems with limited information.

However, the original particle filter is not effective in estimating parameters that change rapidly, such as stiffness degradation, caused by damage to the structure over a short period, such as an earthquake (Lei *et. al.*, 2016). This is because it is assumed that the system parameters do not change with time when the aforementioned artificial noise $\mathbf{w}_{\theta,k}$ is introduced. In other words, the particle filter cannot adapt quickly to the rapid changes in the system parameter, which in turn results in very poor estimation performance.

To address this, Liu *et. al.* (2005) proposed the adaptive particle filter that can adapt quickly to rapid change in the system parameter. It is a modified version of particle filter where the adaptation step is added to algorithm before the measurement update step, as shown in Figure 2.4.

The adaptive particle filter is a method of artificially increasing noise $\mathbf{w}_{\theta,k}$, multiplying by an Adaptive coefficient λ_k that changes over time. That is, the method of artificially increasing the variance of the prior distribution of the system

parameters θ_k at the prediction step to find estimates of θ_k over a wider range.

λ_k increases when the difference between the theoretical measurement $\hat{\mathbf{y}}_k$ obtained from the given measurement equation, Eq. 2.8, and the actual measurement \mathbf{y}_k . That is, when a sudden change in the system occurs, the value of λ_k increases accordingly. λ_k is defined as the following equations.

$$\lambda_0 = \frac{\text{tr}[V_k]}{\text{tr}[M_k]} \quad (2.26)$$

$$\lambda_k = \begin{cases} \lambda_0 & \text{if } \lambda_0 > 1 \\ 1 & \text{if } \lambda_0 \leq 1 \end{cases} \quad (2.27)$$

Here, V_k is the covariance matrix of the actual residual, and M_k is the covariance matrix of the theoretical residual. This shows that λ_k increases when the difference between the theoretical and actual covariance becomes larger. V_k and M_k are defined as the following Eq. 2.28 and Eq. 2.29 respectively.

$$\begin{aligned} V_k &= E \left[\gamma_k^i (\gamma_k^i)^T \right] \\ &\cong \frac{\rho V_{k-1} + \frac{1}{N_p} \sum_{i=1}^{N_p} (y_k - y_{k|k-1}^i) (\gamma_k^i = y_k - y_{k|k-1}^i)^T}{1 + \rho} \\ &= \frac{\rho V_{k-1} + \frac{1}{N_p} \sum_{i=1}^{N_p} \gamma_k^i (\gamma_k^i)^T}{1 + \rho} \end{aligned} \quad (2.28)$$

$$M_k = \frac{1}{kN_p} \sum_{j=0}^{k-1} \sum_{i=1}^{N_p} (\hat{y}_{j+1|j} - y_{j+1|j}^i) (\hat{y}_{j+1|j} - y_{j+1|j}^i)^T \quad (2.29)$$

Here, γ_k^i refers to the actual residual, and $(\hat{y}_{j+l|j} - y_{j+l|j}^i)$ is the theoretical residual. Here, ρ is the forgetting factor and $\rho = 0.95$ is selected generally (Liu *et. al.*, 2005). As shown in Eq. 2.26, V_k is a weighted mean of the covariance matrix of the actual residual and V_{k-1} with the weight equal to ρ . In other word, only portion of V_{k-1} is considered to obtain V_k . In addition, as shown in Eq. 2.29, M_k is the average of the covariance of the actual residual for each particle over all time.

After obtaining λ_k at the time step k , algorithm returns back to the prediction step and propagates the state again with the new artificial noise multiplied by λ_k . That is, $\mathbf{w}_{a,k}$, shown in Eq. 2.14, can be rewritten with the following equation.

$$\mathbf{w}_{a,k} = [\mathbf{w}_k \quad \lambda_k \mathbf{w}_{\theta,k}]^T \quad (2.30)$$

The adaptive particle filter repeats these processes every time step to help algorithm to adapt quickly when the system changes. This method can greatly reduce the bias of estimation, which is the issue of the original particle filter, by estimating θ_k from wide range.

However, as mentioned earlier, the adaptive particle filter cannot consider information of measurement from each degree of freedom because all elements of artificial noise $\mathbf{w}_{\theta,k}$ are multiplied by one constant λ_k expressed with V_k and M_k . In other words, the elements of $\mathbf{w}_{\theta,k}$ estimating system parameters that have

not changed are increased by λ_k . Accordingly, it is inevitable that the increase in overall noise increases the variance of the estimation. To solve this problem, in this study, the modified adaptive particle filter is proposed in Chapter 3, multiplying each element of $\mathbf{w}_{\theta,k}$ by different adaptive coefficients by taking into account the information from each measurement of degree of freedom.

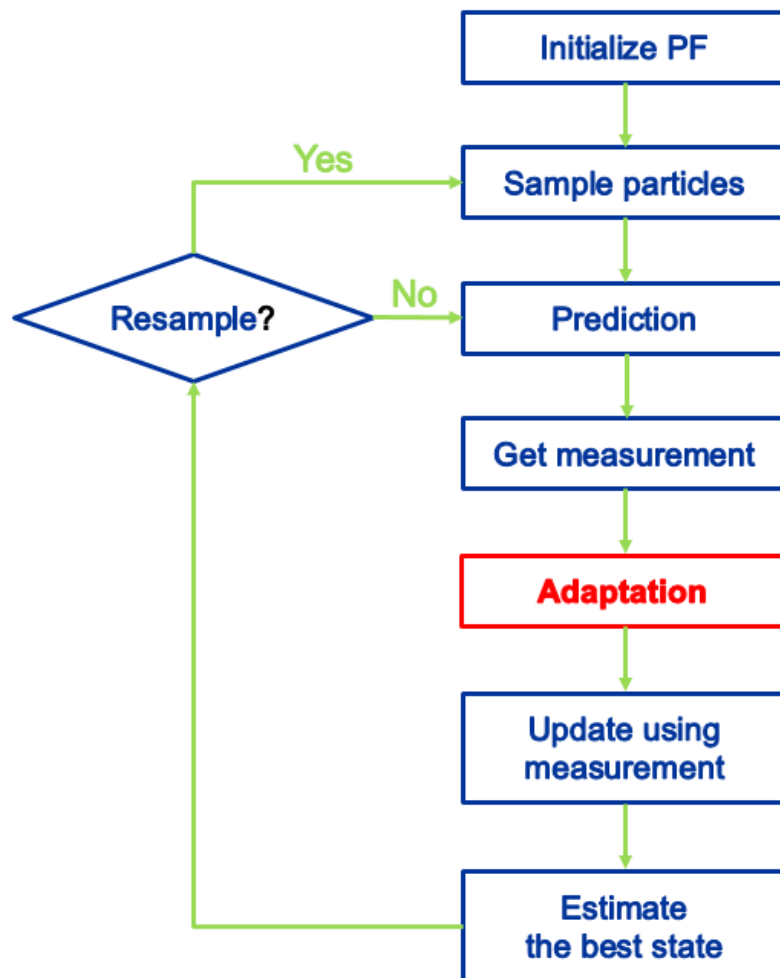


Figure 2.4 Flow chart of adaptive particle filter

3. Proposed Modified Adaptive Particle Filter with Ensemble Learning Method

3.1. Modified Adaptive Particle Filter

As mentioned in section 2.3, the adaptive particle filter, where $\mathbf{w}_{\theta,k}$ is multiplied by the same λ_k at every time step k , has problems in that the information obtained from each degree of freedom through measurement was not fully used and the variance of estimates was greatly increased.

To solve these problems, this study proposes the modified adaptive particle filter. In the original methods, the total parameter estimation noise $\mathbf{w}_{\theta,k}$ was increased by the value of λ_k . In contrast, the proposed method multiplies the different coefficients, with the information obtained from each measurement, by each element of $\mathbf{w}_{\theta,k}$. In other words, the proposed method multiplies the adaptive coefficient vector λ_k of the following equation by each element of $\mathbf{w}_{\theta,k}$ instead of multiplying a single coefficient by whole $\mathbf{w}_{\theta,k}$ as shown in Eq. 2.28.

$$\mathbf{w}_{a,k} = \left[\mathbf{w}_k \quad \lambda_k \otimes \mathbf{w}_{\theta,k} \right]^T \quad (3.1)$$

Here, the symbol of \otimes means element-wise multiplication. The adaptive coefficient vector λ_k is defined as the following equation.

$$\boldsymbol{\lambda}_k = \begin{bmatrix} \Lambda_{1,k} & \cdots & \Lambda_{N_\theta,k} \end{bmatrix}^T \quad (3.2)$$

Here, for $i = 1, \dots, N_{DOF}$ and $j = 1, \dots, N_\theta$, $\Lambda_{j,k}$ is defined as the geometric mean of all $\lambda_{i,k}$ related with the parameter θ_j at time step. $\lambda_{i,k}$ is defined as the following equations.

$$\lambda_{0,i} = \frac{V_k(i, i)}{M_k(i, i)} \quad (3.3)$$

$$\lambda_{i,k} = \begin{cases} \lambda_{0,i} & \text{if } \lambda_{0,i} > 1 \\ 1 & \text{if } \lambda_{0,i} \leq 1 \end{cases} \quad (3.4)$$

$V_k(i, i)$ and $M_k(i, i)$ are the i^{th} diagonal element of V_k and M_k , defined as Eq. 2.26 and Eq. 2.27. That is, this is the ratio of actual and theoretical covariance about i^{th} degree of freedom.

As shown in Eq. 2.26 and Eq. 2.27 used in the original adaptive particle filter, information from all degrees of freedom was considered at once by obtaining trace of the covariance matrix. However, the method proposed in this study obtains the geometric mean of the covariance ratio of each degree of freedom, and multiplies it by the specific noise element that estimates the relevant system parameters. That is, the system information obtained from each degree of freedom is considered only with the related parameter estimation noise elements.

As a simple example, as illustrated in Figure 3.1, the system identification of five degrees of freedom structural system is performed. It is assume that an extreme event caused the degradation at third stiffness element k_3 . Due to the

change in k_3 , responses of some degree of freedom close to k_3 are also changed.

The greater the degree of freedom is adjacent to the k_3 , the greater change in response occurs. That is, the actual responses of second and third degrees of freedom obtained from measurements differ greatly from the theoretical responses obtained from the given system equation. Therefore, $\Lambda_{3,k}$ increasing the specific noise element $w_{3,k}$ that estimates the system parameter k_3 can be obtained as shown in the following equation.

$$\Lambda_{3,k} = \sqrt{\lambda_{2,k} \cdot \lambda_{3,k}} \quad (3.5)$$

Eq. 3.5 means that it is only considered that the information about parameter k_3 obtained from relevant degree of freedom $\lambda_{2,k}$ and $\lambda_{3,k}$. Accordingly, each size of $\Lambda_{j,k}$ is calculated differently in accordance with the degree of change in each system parameter. In other words, elements of $\mathbf{w}_{\theta,k}$ estimating parameters with large change increase largely, but elements of $\mathbf{w}_{\theta,k}$ estimating parameters with small change increase small. Therefore, the proposed method has the advantage in estimating precisely with smaller variance than the original method.

The modified adaptive particle filter proposed in this study also increases the artificial noise similar with the original method. Thereby, the bias of estimates is reduced through widely distributed particles. However, since the methods proposed in this study are also based on the methodology that increase the elements of $\mathbf{w}_{\theta,k}$, there is still problem with increasing uncertainty of the estimation due to the increase in variance. In other words, the estimates from each iteration of the

algorithm may be different every time. In addition, as mentioned in Chapter 1, the accuracy of the estimation is greatly affected by how the user chooses the parameter estimation noise $\mathbf{w}_{\theta,k}$. To solve these problems, the ensemble learning method is adopted to aggregate each estimate from all executable algorithms in Section 3.2 to obtain the final estimate.

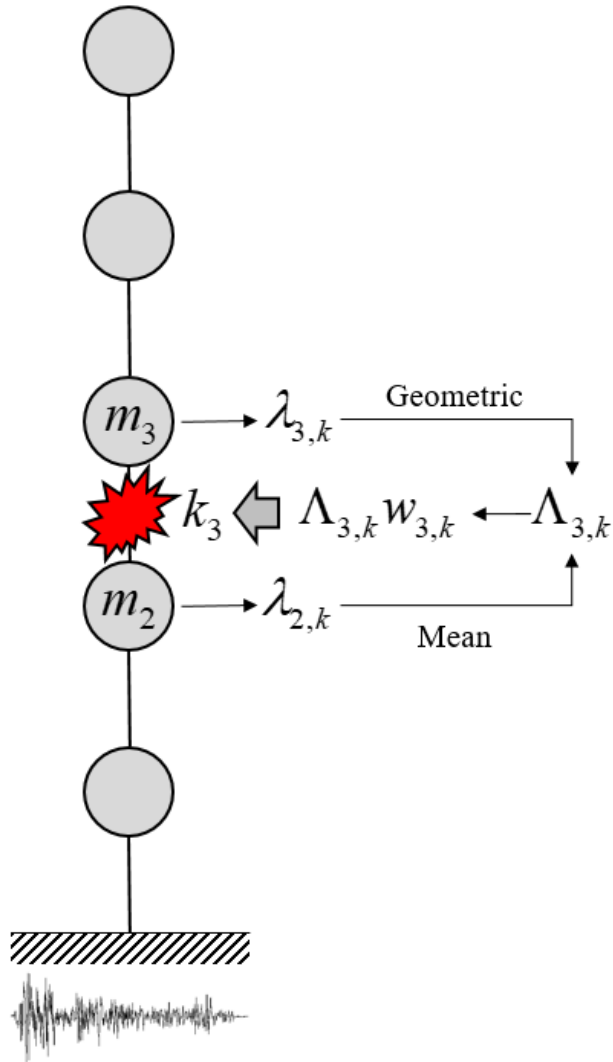


Figure 3.1 Simple example showing how to calculate adaptive coefficient in modified adaptive particle filter

3.2. Ensemble Learning Method

In general, it is difficult for users to have a one model or algorithm that finds optimal solution for the given problem. Even if there is an optimal model within a set of executable algorithms, it is challenging to identify optimal algorithm.

The ensemble learning method is a way to find the final estimate by weighting each estimate from executable algorithms, rather than performing estimation with just one model. A simple diagram of concept of the ensemble learning method is shown in Figure 3.2. Each estimate is taken from executable N algorithms with input x , then the final estimate y is calculated by combining estimates with weights w_n .

For model-based estimation problems, the expected error can be divided into bias and variance terms, as shown in Eq. 3.6.

$$\begin{aligned} E_D \left[\left\{ y(x; D) - h(x) \right\}^2 \right] \\ = \left\{ E_D \left[y(x; D) \right] - h(x) \right\}^2 + E_D \left[\left\{ y(x; D) - E_D \left[y(x; D) \right] \right\}^2 \right] \end{aligned} \quad (3.6)$$

The first term of the right side represents bias, and the second term represents the variance. Here, x , D and y mean input, dataset and exact solution respectively.

The final goal is to minimize the expected errors. However, there is a trade-off relationship between bias and variance. This is called bias-variance tradeoff. That is, flexible models have low bias and high variance, while strict models have high bias and low variance. The optimal model is to have a balance between bias and

variance, which means that the error has minimum value.

In general, the variance of solutions obtained by combining different flexible models using the ensemble learning method are canceled each other (Friedman *et.al.*, 2001). In other word, the combined estimate from ensemble learning method is more accurate and stable than the estimate obtained from a single model.

There are several ways to combine executable models. Among them, the simplest and effective method is to use the average of the estimates obtained in each model as the final estimate. This method is referred to as committee method or bootstrap aggregating (bagging). That is, the bagging method gives equal weight to the estimate from each model, so that all models are considered equally important.

$$y_{COM} = \frac{1}{N} \sum_{n=1}^N y_n \quad (3.7)$$

Here, y_n and y_{COM} are the estimate from a single model and from the bagging method respectively. The bagging method can reduce the variance of estimation and prevent the overfitting by improving unstable procedure. In the bagging, sum of squared error E_{AV} and the mean error E_{COM} can be written as Eq. 3.8 and Eq. 3.9 respectively (Breiman, 1996).

$$E_{AV} = \frac{1}{N} \sum_{n=1}^N E_{\mathbf{x}} \left[\varepsilon_n(\mathbf{x})^2 \right] \quad (3.8)$$

$$E_{COM} = E_{\mathbf{x}} \left[\left\{ \frac{1}{N} \sum_{n=1}^N \varepsilon_n(\mathbf{x}) \right\}^2 \right] \quad (3.9)$$

Here, $\varepsilon_n(\mathbf{x})$ is error between exact solution and estimation. If $\varepsilon_n(\mathbf{x})$ has zero-mean and errors are not correlated with each other, the following equation is valid.

$$E_{COM} = \frac{1}{N} E_{AV} \quad (3.10)$$

However, Eq. 3.10 is not valid in many cases because of the errors are highly correlated with each other generally. Even if the above conditions are not valid, E_{COM} is always smaller than E_{AV} , which means the Bagging can improve the accuracy of the estimation in all cases (Nasrabadi, 2007).

As the modified adaptive particle filter proposed in section 3.1 increases the artificial noise, the bias is decreased but the variance is increased. This is a more flexible model than the original particle filter. Therefore, in order to increase the accuracy of the proposed method in this study, the bagging method is introduced to the modified adaptive particle filter at every time step. In addition, the parameter estimation noise $\mathbf{w}_{\theta,k}$ is randomly selected from the uniform distribution with the range mentioned in Chapter 2, and the modified adaptive particle filter with selected noise is set as an individual algorithm. In time step k , Eq. 3.11 is relationship between $\hat{\mathbf{z}}_{n,k}$, the estimate of the state obtained from an individual model and $\hat{\mathbf{z}}_k$ the final estimate obtained by Bagging.

$$\hat{\mathbf{z}}_k = \frac{1}{N} \sum_{n=1}^N \hat{\mathbf{z}}_{n,k} \quad (3.11)$$

A schematic of the final proposed method is shown in Figure 3.3. $\mathbf{w}_{\theta,k}$ in

each modified adaptive particle filter is set up differently at the initialize step. Then, the estimates are obtain from each algorithm through parallel computing each time step. Finally, the final estimate is obtained through the bagging method. The method proposed in Chapter 3 is demonstrated in Chapter 4 through the numerical example.

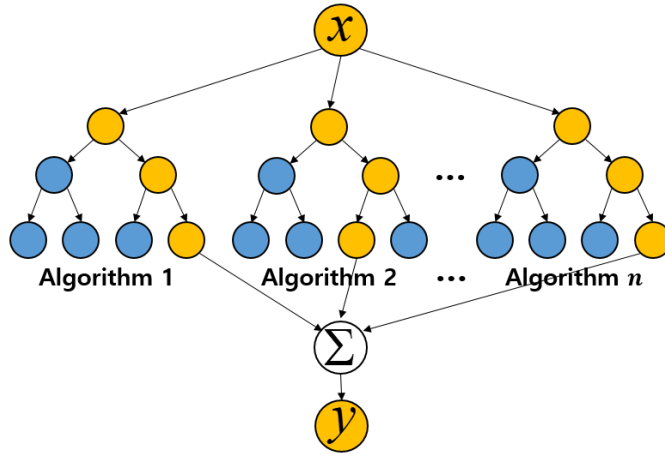


Figure 3.2 Simple concept of ensemble learning method

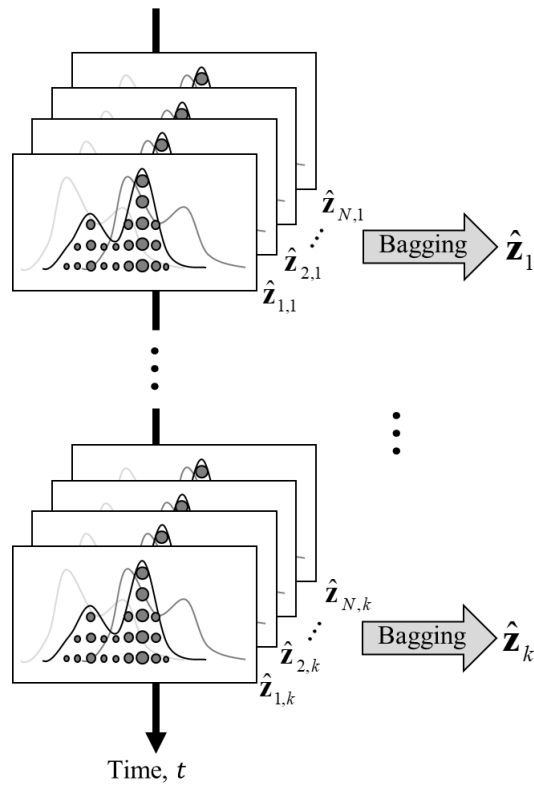


Figure 3.3 Estimation process of modified adaptive particle filter with bagging method

4. Verification of Proposed Method

4.1. Numerical Example

In this section, it is presented that a numerical example to confirm the validity of the methodologies presented in Chapter 3. The target structure is a 10 degree of freedom shear building. It is assumed that local damage in the target structure occurs during the earthquake event using the actual record data of ground acceleration as input data.

4.1.1. Target Structural System

The target structure is a 10 degree of freedom shear building as shown in Figure 4.1. For $i = 1, \dots, 10$, displacement, velocity and acceleration of each degree of freedom is set u_i , \dot{u}_i and \ddot{u}_i . The ground acceleration presented in the section 4.1.2 is set to \ddot{u}_g . The structural properties of each degree of freedom, mass, damping coefficient, and stiffness are set as $m_1, \dots, m_{10} = 100 \text{ kg}$, $c_1, \dots, c_{10} = 5 \text{ N-s/m}$ and $k_1, \dots, k_{10} = 180 \text{ N/m}$ respectively.

When the seismic force is applied to the structure, the seismic force is written as $\mathbf{F}(t) = -\mathbf{M}\ddot{u}_g$. Accordingly, the equation of motion for the target structure is the following equation in the earthquake event (Jia, 2014).

$$\mathbf{M}\ddot{\mathbf{u}}(t) + \mathbf{C}\dot{\mathbf{u}}(t) + \mathbf{K}\mathbf{u}(t) = -\mathbf{M}\ddot{\mathbf{u}}_g \quad (4.1)$$

Here, \mathbf{M} , \mathbf{C} and \mathbf{K} are mass, damping and stiffness matrix, presented in the following Eq. 4.2, Eq. 4.3 and Eq. 4.4 respectively.

$$\mathbf{M} = \text{diag}[m_1 \cdots m_{10}] = \begin{bmatrix} m_1 & & \\ & \ddots & \\ & & m_{10} \end{bmatrix} \quad (4.2)$$

$$\mathbf{C} = \begin{bmatrix} c_1 + c_2 & -c_2 & & & \\ -c_2 & c_2 + c_3 & -c_3 & & \\ & & \ddots & & \\ & & & -c_9 & c_9 + c_{10} & -c_{10} \\ & & & & -c_{10} & c_{10} \end{bmatrix} \quad (4.3)$$

$$\mathbf{K} = \begin{bmatrix} k_1 + k_2 & -k_2 & & & \\ -k_2 & k_2 + k_3 & -k_3 & & \\ & & \ddots & & \\ & & & -k_9 & k_9 + k_{10} & -k_{10} \\ & & & & -k_{10} & k_{10} \end{bmatrix} \quad (4.4)$$

To estimate Eq. 4.1 using the Particle Filter in the time domain, state is set to displacement \mathbf{u} and $\dot{\mathbf{u}}$ velocity. The state vector $\mathbf{z}(t)$ is shown in Eq.4.5. In addition, the system parameters to be estimated in this study are set to all stiffness \mathbf{k} . The augmented state vector $\mathbf{z}_a(t)$ can be written as Eq. 4.6.

$$\mathbf{z}(t) = [\mathbf{u}(t) \quad \dot{\mathbf{u}}(t)] = [u_1 \cdots u_{10} \quad \dot{u}_1 \cdots \dot{u}_{10}] \quad (4.5)$$

$$\mathbf{z}_a(t) = [\mathbf{z}(t) \quad \mathbf{k}(t)] = [\mathbf{u}(t) \quad \dot{\mathbf{u}}(t) \quad k_1, \cdots, k_{10}]^T \quad (4.6)$$

$\mathbf{z}_a(t)$ in Eq. 4.6 is used as the state of the Particle Filter to perform the

estimation. Then, the equation of motion in Eq. 4.1 is expressed as the nonlinear function in the state-space representation.

$$\dot{\mathbf{z}}_a = f(\mathbf{z}_a, \ddot{\mathbf{u}}_g, \mathbf{w}_a) \quad (4.7)$$

Here, \mathbf{w}_a is the augmented noise vector in which the parameter estimation noise \mathbf{w}_θ is attached to the noise \mathbf{w} for $\mathbf{z}(t)$, as Eq. 4.8.

$$\mathbf{w}_a = [\mathbf{w} \quad \mathbf{w}_\theta]^T \quad (4.8)$$

Acceleration from all degree of freedom are measurement, and measurement equation is the following Eq. 4.9. The measurement update in every time step is performed by comparing the theoretical measurement \mathbf{y} as shown in Eq. 4.9, using \mathbf{u} , $\dot{\mathbf{u}}$ and \mathbf{k} from $\mathbf{z}_a(t)$, with the actual measurement $\hat{\mathbf{y}}$.

$$\mathbf{y} = \ddot{\mathbf{u}} = -\mathbf{M}^{-1}\mathbf{C}\dot{\mathbf{u}} - \mathbf{M}^{-1}\mathbf{K}\mathbf{u} - \ddot{\mathbf{u}}_g \quad (4.9)$$

4.1.2. Ground Acceleration

The ground acceleration used as input is the N-S component of the El Centro earthquake that occurred in the Imperial Valley in 1940. It was the first major earthquake to be recorded by a strong-motion seismograph located next to a fault rupture. For this reason, El Centro earthquake is one of the most commonly used seismic record in many related studies.

The El Centro earthquake recorded 0.3g of the Peak Ground Acceleration

(PGA), and 6.9 of moment magnitude. It was recorded as the largest earthquake to hit the Imperial Valley. The measurement frequency is 50 Hz, i.e. observed every 0.02 s. The raw acceleration record is as shown in Figure 4.2 (Chopra, 2017).

4.1.3. Stiffness Degradation

To test the performance of proposed modified adaptive particle, it is assumed that severe stiffness degradation occurs in stiffness k_1 , k_2 and k_3 , as shown in Figure 4.3,.

The reason why stiffness degradation occurs in 1st, 2nd and 3rd floor of the building, Dya *et. al.* (2015) verified that the vulnerability index in these floors was significantly higher than other floors. This means that first, second and third floor are more vulnerable to earthquakes than other floors.

It is assumed that k_1 is degraded from 180 N/m to 150 N/m, then degraded to 120 N/m at 10 sec and 20 sec respectively. A severe degradation in k_2 occurs at 10 sec, which is decreased from 180 N/m to 130 N/m. k_3 is degraded from 180 N/m to 140 N/m at 15 sec. The process of degradation is shown in Figure 4.3. This pattern of degradation is more exaggerated than real data. The reason for this setting is to verify that the proposed methodology well estimates in these extreme situations.

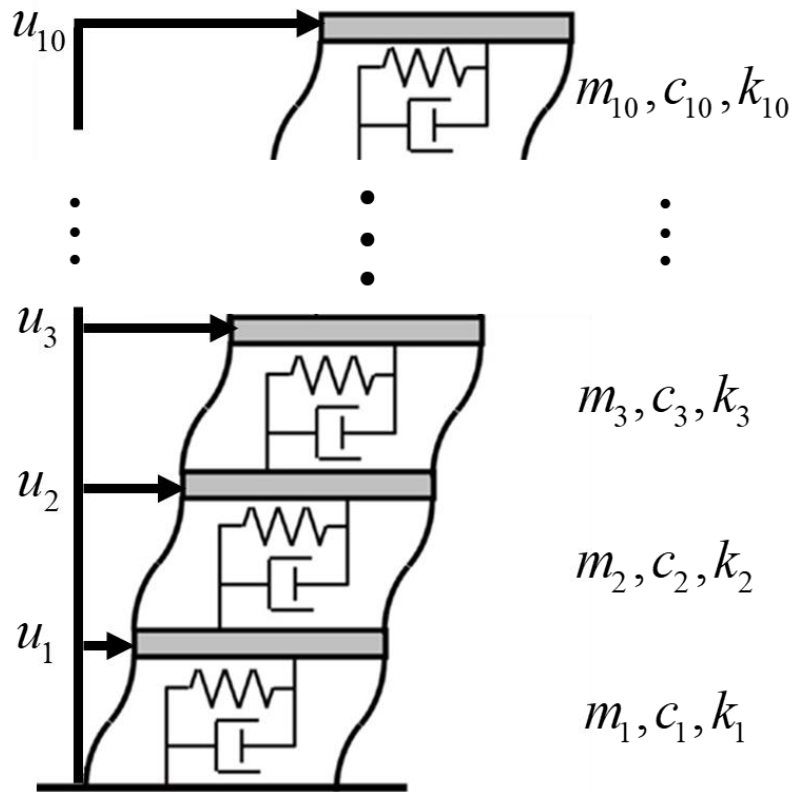


Figure 4.1 Target Structure (10 story shear building)

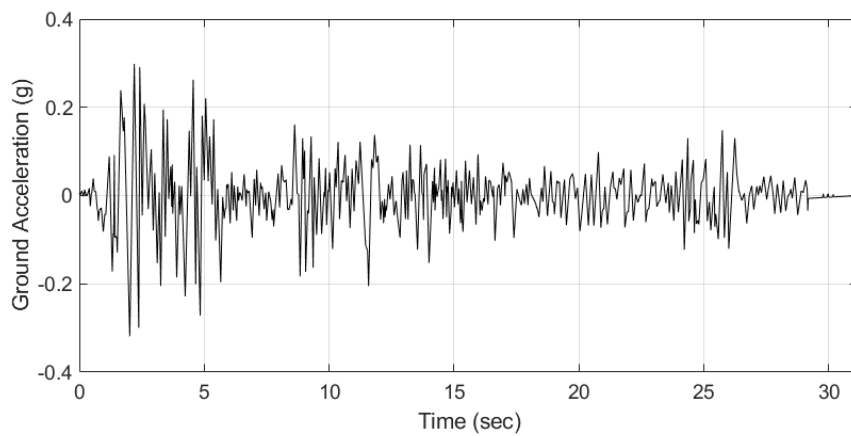


Figure 4.2 Ground acceleration record of El Centro earthquake

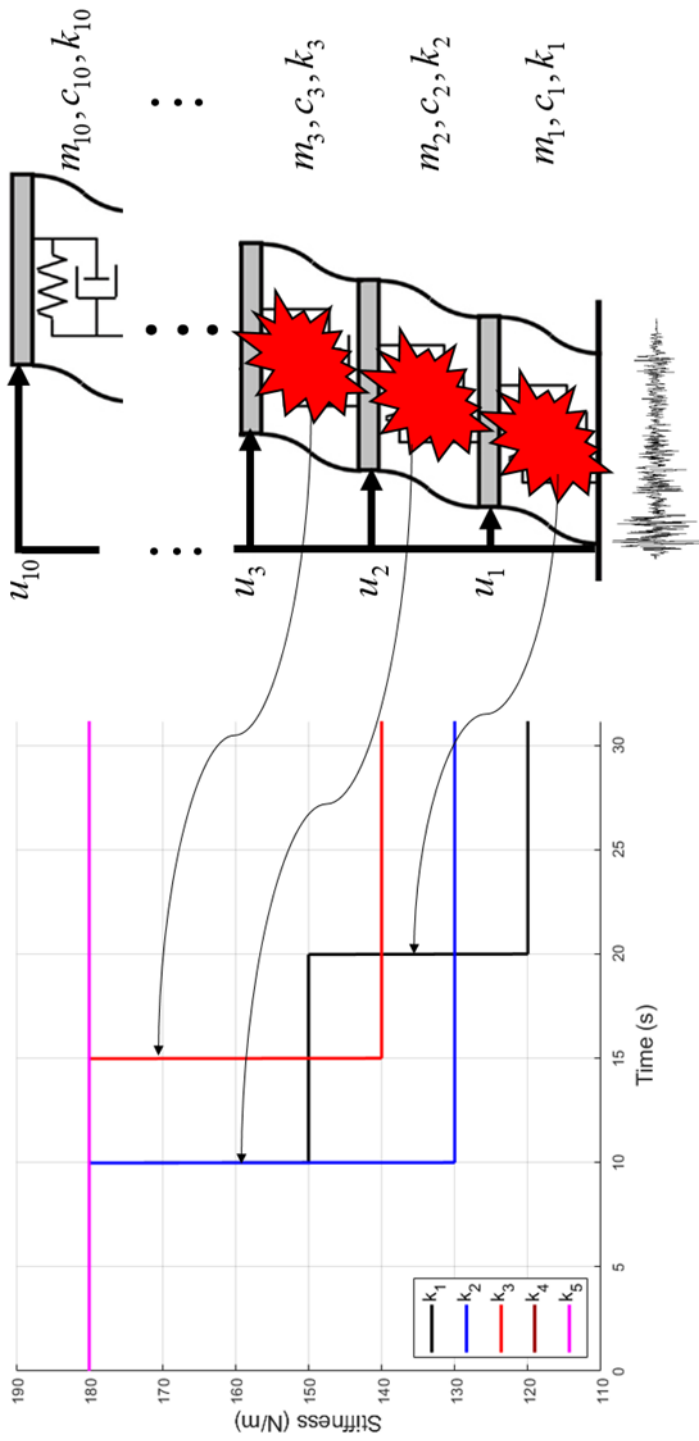


Figure 4.3 Stiffness degradation in k_1 , k_2 and k_3

4.2. Verification Results and Discussion

In this section, the result of the original Particle Filter, shown in Chapter 2, for the numerical example of Section 4.1 is presented. After that, the proposed method is verified by comparing the results of modified adaptive particle filter without and with the bagging method with the result of original particle filter.

The number of particles N_p of all particle filter algorithms is set to $N_p = 20,000$. The initial value of state \mathbf{u} and $\dot{\mathbf{u}}$ is zero and of all parameters \mathbf{k} is 175 N/m.

When a single algorithm is used (sections 4.2.1 and 4.2.2), the distribution of parameter estimation noise \mathbf{w}_θ is assumed to be all $N(0, 10^{-2})$ (i.e. Gaussian noise). The standard deviation of the distribution is set to about 0.1% of the initial value of parameters. In case of using the bagging method in Section 4.2.3, total 300 parallel algorithms are used. The standard deviation of \mathbf{w}_θ in each algorithm is randomly sampled from uniform distribution $U(10^{-1}, 10^0)$, and each is assumed to be Gaussian noise.

4.2.1. Original Particle Filter

The results of the original particle filter, which is fundamental algorithm of this study, are shown in Figure 4.4 and Figure 4.5. Figure 4.4 shows the estimated displacement, velocity, and acceleration of degree of freedom 1 and 10,

respectively. Figure 4.5 shows the estimated results for the system parameters $k_1 \sim k_5$ and $k_6 \sim k_{10}$ respectively.

As mentioned in Chapter 2, the original particle filter assumes that the system parameters do not change over time. Because of this, the standard deviation of parameter estimation noise \mathbf{w}_θ is set to be quite small. Therefore, the particle filter estimates over a narrow range.

However, the numerical example in this study assumes that the system parameters changes considerably at the certain time. Therefore, as shown in Figure 4.5, estimates of all parameters at 10 sec, when the first occurrence of the stiffness degradation occurs, are significantly inaccurate. It is shown that estimates of the state and acceleration in Figure 4.4 also become increasingly inaccurate after 10 sec.

From the results in Figure 4.5, it can be seen that the convergence rate of the estimation of $k_1 \sim k_3$, where sudden change occurs, is significantly slow due to the small estimation noise. Because of this, there is difference between the theoretical measurement in Eq. 4.9 and the actual measurement. To reduce this difference, it can be seen that estimates of other parameters are also decreased. In other words, small estimation noise results in estimation being caught on the local minima, which differs from the exact solution. Even if an estimation is performed for a longer time, an inaccurate estimate continue and the difference between the theoretical and the actual measurement become larger which means divergence of estimation.

4.2.2. Modified Adaptive Particle Filter

When estimating parameters that change over time, the fundamental problem with original particle filter is that it uses small parameter estimation noise that does not change over time. To address this, this study proposes modified adaptive particle filter, which is improved version of adaptive particle filter in constructing the adaptive coefficient vector.

The results of the modified adaptive particle filter proposed in this study are shown in Figure 4.6 and Figure 4.7. As with the results of the original particle filter, Figure 4.6 is the result of estimation of the displacement, velocity and acceleration of degree of freedom 1 and 10, and Figure 4.7 is the estimation result of the system parameters, respectively.

Comparing the results from Figure 4.6 and Figure 4.7 with those from the original particle filter shows a significant improvement in estimation accuracy. In particular, modified adaptive particle filter adapts quickly at the time when the stiffness degradation occurs, and that parameter estimates converges to the exact solution. The state and acceleration estimates are also almost same with the exact solution for all times.

The improvement in accuracy is due to the adaptive coefficient vector λ_k proposed in Eq. 3.1 through Eq. 3.4. For $i = 1, \dots, 5$, Figure 4.8 shows the change of the adaptive coefficient $\lambda_{i,k}$ proposed in Eq. 3.3 and Eq. 3.4 over time. As shown in Figure 4.8, the value of $\lambda_{i,k}$ obtained from the relevant degree of freedom increases when stiffness degradation occurs in any system parameter. In

addition, the value of $\lambda_{i,k}$ related to time-invariant parameters does not change much. From these results, it is confirmed that the modified adaptive particle filter increases each element of parameter estimation noise $w_{\theta_i,k}$ differently using the geometric mean $\Lambda_{j,k}$ of related $\lambda_{i,k}$.

However, as shown in Figure 4.7, the bias in estimates is decreased significantly compared to the results of the original particle filter, but the variance is increased significantly. In particular, estimates of parameters where stiffness degradation does not occur vary significantly. As mentioned earlier, this is because the modified adaptive particle filter is based on increase of parameter estimation noise. As shown in Figure 4.8, even $\lambda_{i,k}$ related to time-invariant parameters have a value of more than one in many period. In other words, the variance of estimation increases in whole estimation time. In particular, all $\lambda_{i,k}$ have a greater value than the other duration from the time the stiffness degradation occurred until the estimates are converged. This is shown in the lower graph in Figure 4.7, showing a significant increase in variance of parameter estimation that does not change.

Thus, there is possibility to reduce the estimation error, and of introducing the modified adaptive particle filter with the bagging method, which is final proposed method in this study.

4.2.3. Modified Adaptive Particle Filter with Bagging

As mentioned in the previous section, the modified adaptive particle filter

decreases the bias in estimation due to the introduction of adaptive coefficient. However, the variance of estimation is increased significantly. To solve this problem, the bagging method, which is one of the ensemble learning methods, is applied to modified adaptive particle filter in this study.

The results of parameter estimation for modified adaptive particle filter with the bagging method are shown in Figure 4.9. As shown in Figure 4.7 in the previous section, the upper graph is the estimation result of $k_1 \sim k_5$, and the lower graph is the estimation result of $k_6 \sim k_{10}$.

Comparing the results of Figure 4.9 and Figure 4.7, it shows a significant reduction in variance in all time, with no significant change in bias. In particular, as shown in Figure 4.7, due to increased parameter estimation noise at the time of stiffness degradation, the variance of estimation of time-invariant parameters is increased greatly. In comparison, Figure 4.9 shows that the variance of estimation of time-invariant parameters is noticeably reduced. This verifies the validity of the modified adaptive particle Filter with the bagging methodology.

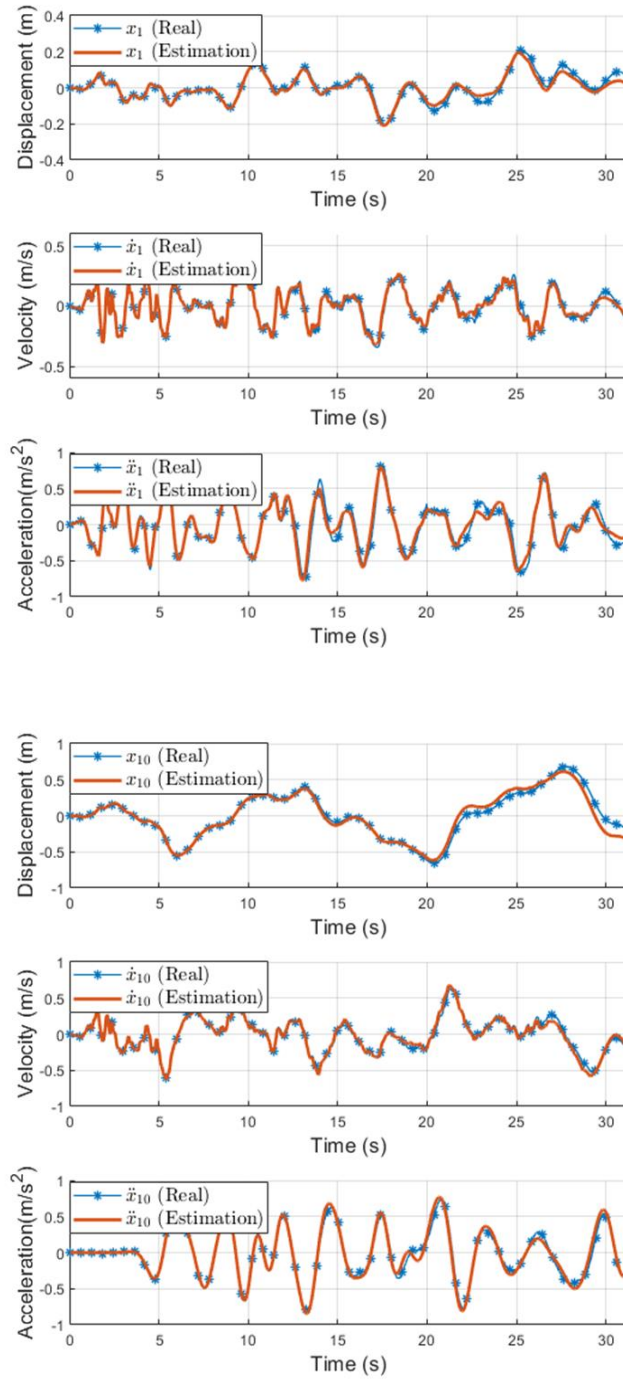


Figure 4.4 Displacement, velocity and acceleration estimation of degree of freedom 1 (upper) and 10 (lower) from particle filter

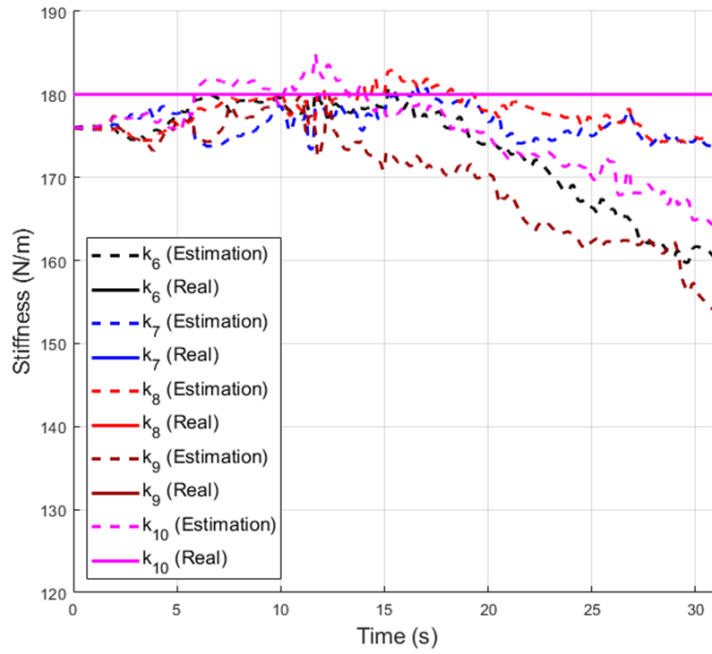
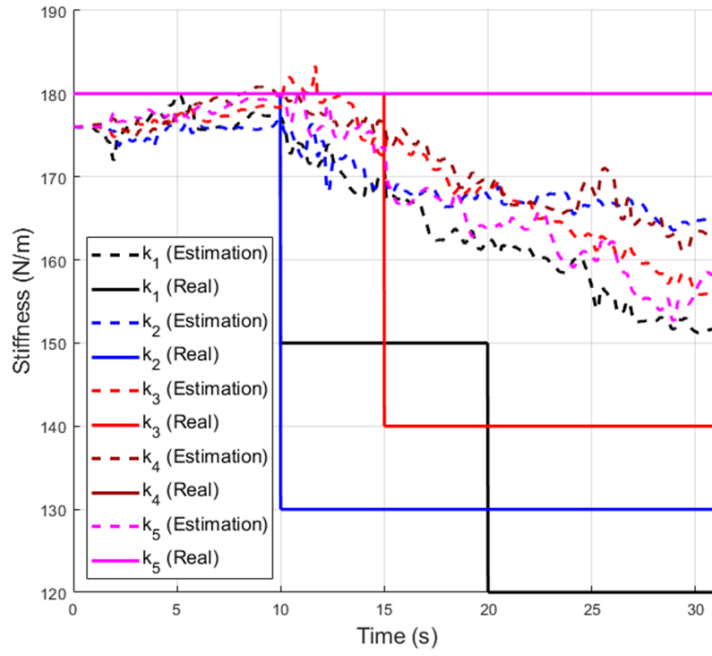


Figure 4.5 Parameter estimation of $k_1 \sim k_5$ (upper) and $k_6 \sim k_{10}$ (lower) from particle filter

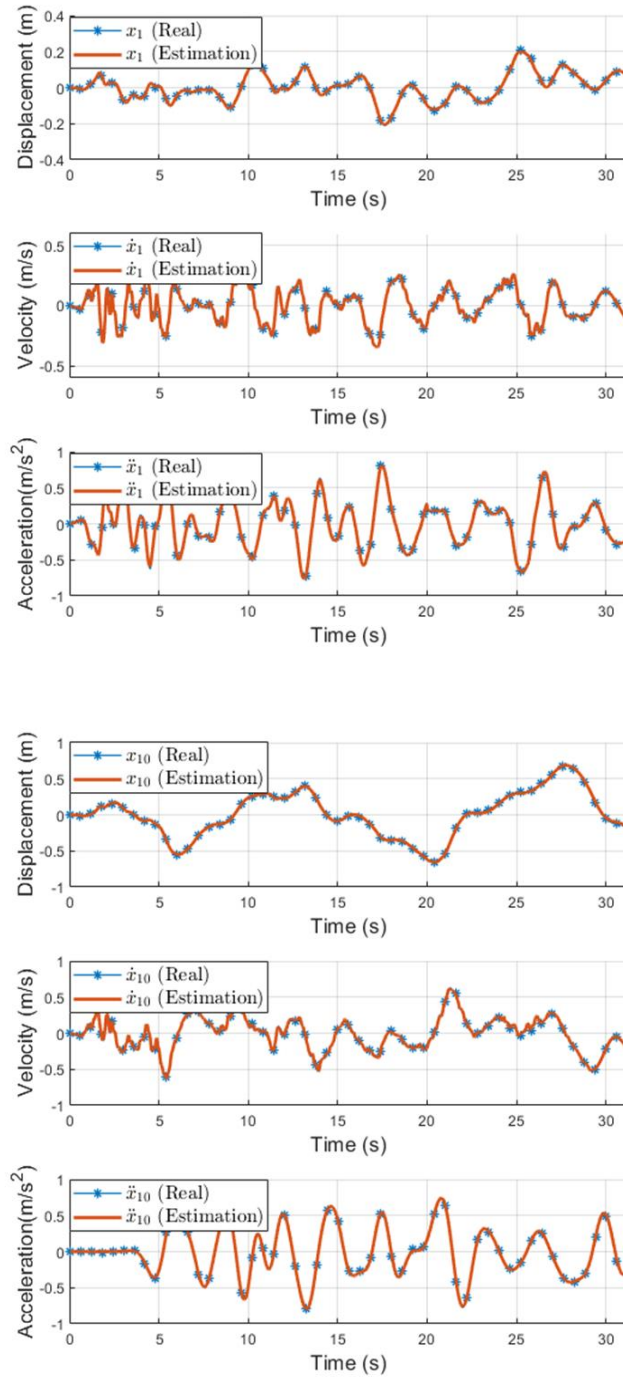


Figure 4.6 Displacement, velocity and acceleration estimation of degree of freedom 1 (upper) and 10 (lower) from modified adaptive particle filter

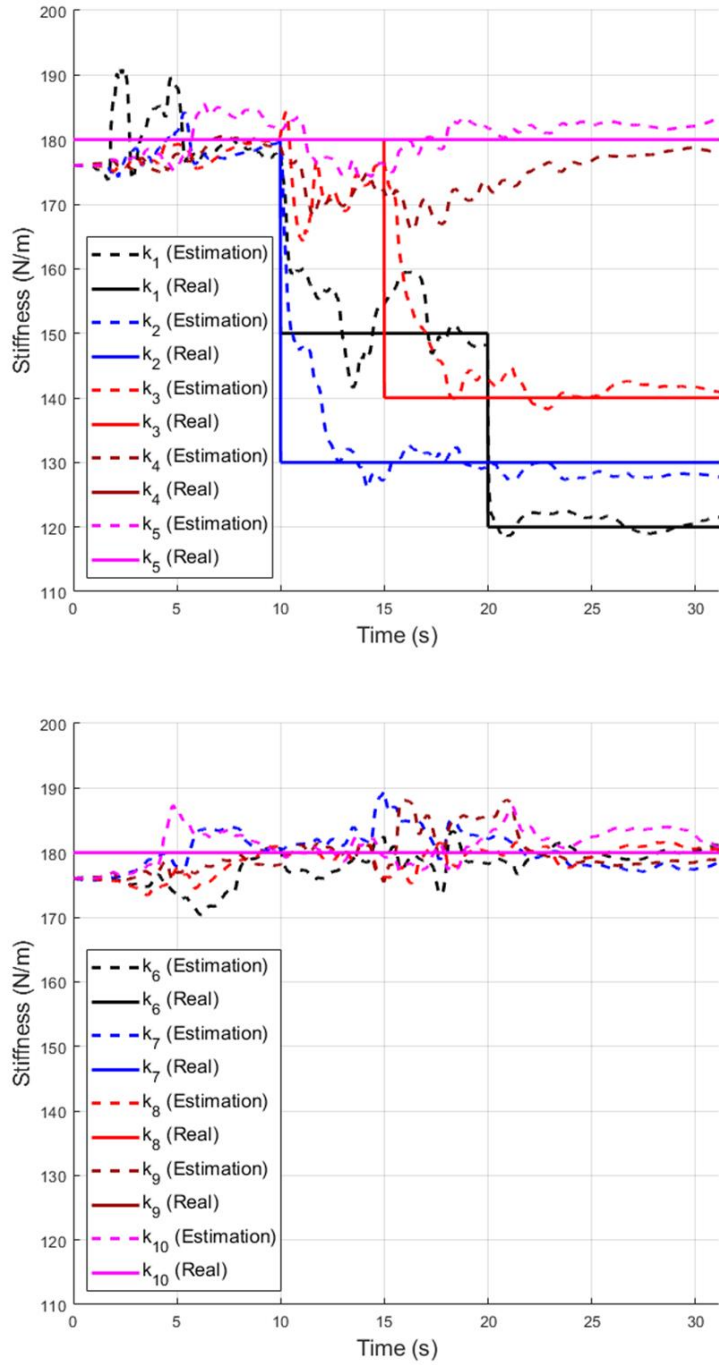


Figure 4.7 Parameter estimation of $k_1 \sim k_5$ (upper) and $k_6 \sim k_{10}$ (lower) from modified adaptive particle filter

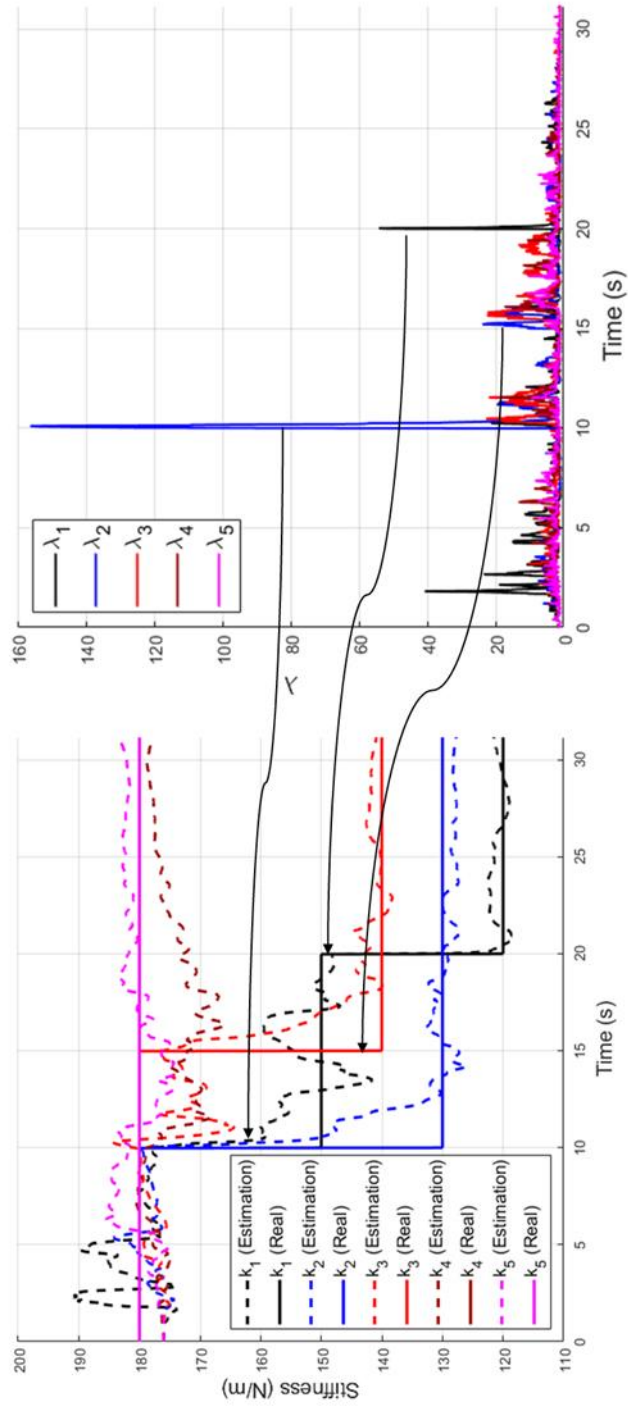


Figure 4.8 Change in values of $\lambda_{t,k}$ over time

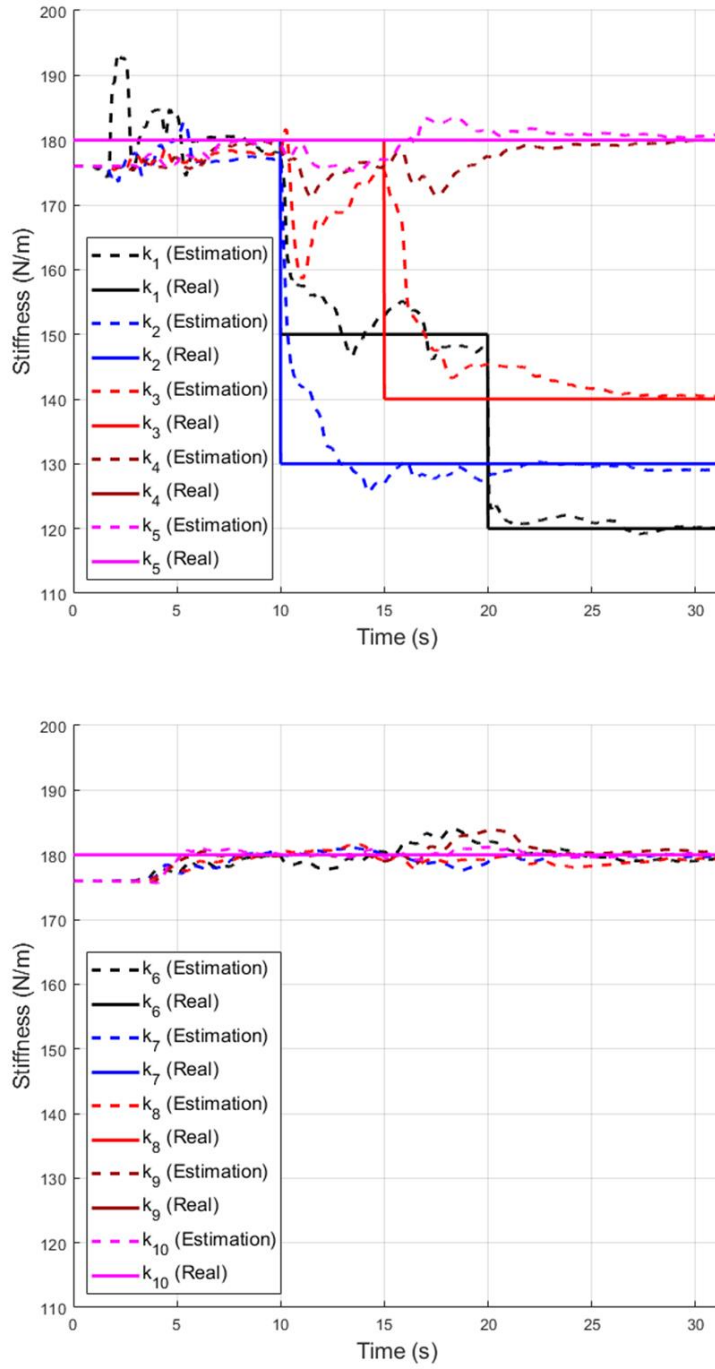


Figure 4.9 Parameter estimation of $k_1 \sim k_5$ (upper) and $k_6 \sim k_{10}$ (lower) from modified adaptive particle filter with bagging method

5. Conclusion

In this study, modified adaptive particle filter is introduced to estimate the sudden change in system parameters that occur during extreme events such as earthquakes. It is confirmed that changes in parameters, such as stiffness degradation, can be detected only with a small amount of measurement data and simple calculations over time with considerable accuracy comparing with the original particle filter. In addition, the variation of estimation increased by introducing of adaptive coefficient was greatly reduced by applying the ensemble learning method, the bagging method in this study.

There are four major further studies based on this study. First, effective algorithm that requires lower computational effort can be developed by improving algorithm. The particle filter requires a significant amount of computational effort comparing with Kalman filter-based methodology. If the proposed method in this study is used in devices with low computational capacity, it will take considerable calculation time.

Second is to improve the methodology to achieve high accuracy in nonlinear systems. In general, many infrastructure have high nonlinearity. However, this study only addressed estimation of a linear structure. Therefore, the methodology proposed in this study can be improved for nonlinear system.

Third is to improve the methodology so that it can be estimated with small number of measurements. In this study, acceleration obtained from all degrees of freedom were used as measurement. However, the measurement can be obtained

only from about 5% of degree of freedom in practice. Therefore, it is essential to ensure accurate estimation with less measurement.

Finally, the correlation between degree of freedom can be considered to construct the adaptive coefficient vector. In this study, the adaptive coefficient vector was constructed by simply geometric average the degree of freedom associated with specific parameter. In other words, the correlation between degrees of freedom was assumed to be zero. However, there is correlation between all degrees of freedom. Considering this, a more accurate estimation would be possible.

Further studies based on results of this study are expected to enhance the effective post-evaluation. Accordingly, it is possible to establish the monitoring methodologies through indirect estimation that is more effective than the existing method.

Reference

- Alvin, K. F., Robertson, A. N., Reich, G. W., & Park, K. C. (2003). Structural system identification: from reality to models. *Computers & structures*, 81(12), 1149-1176.
- Ang, A. H. S., & Tang, W. H. (2007). *Probability concepts in engineering: emphasis on applications in civil & environmental engineering* (Vol. 1). New York: Wiley.
- Bisht, S. S., & Singh, M. P. (2014). An adaptive unscented Kalman filter for tracking sudden stiffness changes. *Mechanical Systems and Signal Processing*, 49(1-2), 181-195.
- Breiman, L. (1996). Bagging predictors. *Machine learning*, 24(2), 123-140.
- Candy, J. V. (2016). *Bayesian signal processing: classical, modern, and particle filtering methods* (Vol. 54). John Wiley & Sons.
- Chatzi, E. N., & Smyth, A. W. (2009). The unscented Kalman filter and particle filter methods for nonlinear structural system identification with non-collocated heterogeneous sensing. *Structural Control and Health Monitoring: The Official Journal of the International Association for Structural Control and Monitoring and of the European Association for the Control of Structures*, 16(1), 99-123.
- Chopra, A. K. (2017). Dynamics of Structures. Theory and Applications to. *Earthquake Engineering*.

- Dya, A. F. C., & Oretaa, A. W. C. (2015). Seismic vulnerability assessment of soft story irregular buildings using pushover analysis. *Procedia Engineering*, 125, 925-932.
- Friedman, J., Hastie, T., & Tibshirani, R. (2001). *The elements of statistical learning* (Vol. 1, No. 10). New York, NY, USA:: Springer series in statistics.
- Images from the Sichuan earthquake part 5. (2009, March 30). Retrieved January 22, 2019, from AGU Blogosphere: <https://blogs.agu.org/landslideblog/2009/03/30/images-from-the-sichuan-earthquake-part-5-xingyiu/>
- Jia, J. (2014). *Essentials of applied dynamic analysis*. Springer Berlin Heidelberg.
- Lei, Y., Zhou, H., & Lai, Z. L. (2016). A computationally efficient algorithm for real-time tracking the abrupt stiffness degradations of structural elements. *Computer-Aided Civil and Infrastructure Engineering*, 31(6), 465-480.
- Liu, M., Zang, S., & Zhou, D. (2005). Fast leak detection and location of gas pipelines based on an adaptive particle filter. *International Journal of Applied Mathematics and Computer Science*, 15(4), 541.
- Ljung, L. (1979). Asymptotic behavior of the extended Kalman filter as a parameter estimator for linear systems. *IEEE Transactions on Automatic Control*, 24(1), 36-50.
- Nasrabadi, N. M. (2007). Pattern recognition and machine learning. *Journal of electronic imaging*, 16(4), 049901.
- Simon, D. (2006). *Optimal state estimation: Kalman, H infinity, and nonlinear approaches*. John Wiley & Sons.

- Staff and agencies. (2017, November 16). *South Korea earthquake: Tremors that rocked Pohang were second-strongest on record*. Retrieved January 22, 2019, from <https://www.independent.co.uk/news/world/asia/south-korea-earthquake-latest-pohang-quake-second-strongest-record-5-4-magnitude-a8057946.html>
- Wan, E. A., & Van Der Merwe, R. (2000). The unscented Kalman filter for nonlinear estimation. In *Adaptive Systems for Signal Processing, Communications, and Control Symposium 2000*. AS-SPCC. The IEEE 2000 (pp. 153-158). Ieee.
- Yang, J. N., Lin, S., Huang, H., & Zhou, L. (2006). An adaptive extended Kalman filter for structural damage identification. *Structural Control and Health Monitoring: The Official Journal of the International Association for Structural Control and Monitoring and of the European Association for the Control of Structures*, 13(4), 849-867.

국문 초록

적응형 파티클 필터와 앙상블 학습 기법을 이용한 지진동 응답 기반 구조 시스템 파라미터 추정

김 민 규

경주·포항 지진 발생 이후 사회 기반 시설에 대한 정확한 사후 평가와 모니터링에 대한 사회적 요구가 점차 증가하고 있다. 정확도를 높이기 위해선 시스템 방정식, 즉 시스템 파라미터의 정확한 추정을 통한 시스템 식별이 필수적이다. 그러나, 시스템 파라미터를 직접 추정하는 방법은 많은 시간과 비용이 소요되어, 재난 재해 시 빠른 대처가 불가능하다. 따라서, 제한된 데이터로 시스템을 추정하는 간접 추정 방법이 개발되어왔다.

이를 위해 많은 연구에서 자료 동화에 기반한 기계 학습 방법, 그 중에서도 비선형성이 강한 시스템을 추정하기 위해 개발된 파티클 필터를 사용했다. 파티클 필터는 샘플링에 기반하기 때문에 시스템 파라미터 추정에서 높은 정확도를 달성했다. 그러나, 지진과 같은 극한 상황 중에 발생하는 강성 열화와 같은 구조물의 손상은 시스템 파라미터의 갑작스런 변화를 야기할 수 있다. 이러한 상황에서 기존의

파티클 필터 방법은 시스템 파라미터가 시간에 따라 일정하다고 가정하기 때문에, 추정 성능이 떨어진다는 단점이 있다.

선행 연구에서 급격히 변화하는 시스템 파라미터를 기존 파티클 필터에 비해 정확하게 추정하기 위해 적응형 파티클 필터를 개발하였다. 적응형 파티클 필터는 강성 열화와 같이 시간이 따라 변하는 시스템 파라미터를 추정하기 위해, 상황에 따라 인위적으로 파티클 필터의 파라미터 추정 노이즈를 증가시키는 상수를 도입하여 파티클 필터의 수렴 속도를 증가시킨 추정 방법이다. 본 연구에선, 선행 연구 방법을 발전시켜, 각 자유도에서 얻은 측정치를 기반으로 각각의 파라미터 추정 노이즈에 다른 상수값을 할당하는 수정 적응형 파티클 필터를 제안하고자 한다.

그러나 적응형 파티클 필터는 추정의 편향은 감소하지만 파라미터 추정 노이즈의 증가로 인해, 추정의 분산이 증가하는 문제점을 가지고 있다. 이를 해결하기 위해, 본 연구는 사용 가능한 각각의 병렬 알고리즘에서 각각 얻은 추정치를 조합하여 최종 추정치를 구하는 앙상블 학습법을 도입했다. 그 중에서, 병렬 알고리즘에서 동일한 가중치로 추정치를 조합하여 최종 추정치를 얻는 Bootstrap Aggregating 또는 Bagging 방법을 도입하여 추정의 분산을 감소시키는 방법론을 제안한다.

본 연구에서 제안한 방법을 통해, 보다 정확하고 효과적인 사후 평가 및 모니터링이 수행될 수 있을 것이며, 구조물의 손상에 대한

정확한 진단을 통해 구조물의 응답과 같은 제한된 정보만으로 효과적인
유지관리 및 보수가 가능할 것으로 기대된다.

주요어: 지진 재해, 구조물 응답, 시스템 식별, 자료 동화, 적응형 파티클
필터, 앙상블 학습법

학번: 2017-20456